

## The Adsorption Structure of NO on Pd(111) at High Pressures Studied by STM and DFT

Ronnie T. Vang, Jian-Guo Wang, Jan Knudsen, Joachim Schnadt, Erik Lægsgaard, Ivan Stensgaard, and Flemming Besenbacher\*

*Interdisciplinary Nanoscience Center (iNANO) and Department of Physics and Astronomy, University of Aarhus, DK-8000 Aarhus C, Denmark*

*Received: May 13, 2005; In Final Form: June 23, 2005*

Using a combination of scanning tunneling microscopy (STM) and density functional theory (DFT) calculations, we study the adsorption structure of NO on Pd(111) at pressures of up to 720 Torr. From atomically resolved STM images, we identify, at high pressures, only the  $(2 \times 2)$ -3NO structure, which is identical with the highest NO-coverage structure found at low pressure and low temperature. DFT calculations confirm that the  $(2 \times 2)$ -3NO structure is indeed the most stable adsorption structure at high pressures. Contrary to recent suggestions in the literature, we therefore conclude that we find no evidence for a  $(3 \times 3)$ -7NO structure on Pd(111) at high NO pressure.

The adsorption of gas molecules on metal surfaces is at the very heart of heterogeneous catalysis, and the study of adsorption structures on single-crystal surfaces is fundamental to the understanding of catalytic systems. Therefore, numerous adsorption structure studies have been carried out in the past, and an enormous insight has been gained into the structures formed by most gases on clean metal surfaces at standard ultrahigh vacuum (UHV) conditions.<sup>1</sup> However, it has been argued that the structures found under standard surface science conditions (low temperatures and low pressures) might not resemble those found at typical reaction conditions (high pressures and high temperatures), and the existence of a so-called pressure gap has been discussed.<sup>2</sup> Such a pressure gap may occur as a consequence of a kinetic hindrance that does not allow for the thermodynamic favorable structure to form at very low temperatures, or entropic effects can lead to the stabilization of new structures at higher temperatures. These effects are difficult to fully take into account when extrapolating UHV results to the relevant reaction conditions. Experimental input is therefore needed in order to elucidate which adsorption structures are the ones of technological interest for a given reaction.

Several techniques are available for exploring adsorption structures at high gas pressure such as scanning tunneling microscopy (STM),<sup>3–8</sup> transmission electron microscopy (TEM),<sup>9</sup> X-ray diffraction spectroscopy (XDS),<sup>10</sup> sum-frequency generation (SFG),<sup>11</sup> and polarization modulation infrared reflection absorption spectroscopy (PM-IRAS).<sup>12</sup> Recently, we have demonstrated the capability of STM to resolve the adsorption structures formed by CO on Pt(111)<sup>4,5</sup> and Pt(110),<sup>3</sup> and H<sub>2</sub> on Cu(110)<sup>8</sup> surfaces at nearly atmospheric pressures. For all systems, it was shown that the structures found at elevated pressures were identical to structures formed at lower pressures and lower temperatures (i.e., no indications of a pressure gap were revealed for these systems). However, in electrochemical experiments, high adsorbate coverages have been observed,

which cannot be reproduced at low-pressure conditions,<sup>13</sup> high oxygen pressures are for certain systems found to lead to the formation of oxide structures,<sup>6,14,15</sup> and high adsorbate coverage can cause a segregation of the more reactive of the components of a surface alloy.<sup>16,17</sup> One system that displays a true pressure gap, meaning that new adsorption structures are formed on a pure metal at elevated pressures, which are not formed at lower pressures and temperatures, is the NO/Rh(111) adsorption system as reported by Rider et al., who identified a  $(3 \times 3)$ -7NO adsorption structure, which forms in equilibrium with the gas phase only at elevated NO pressures.<sup>7</sup>

In a very recent publication, Ozensoy et al. suggest the existence of a similar pressure gap for NO adsorption on Pd(111).<sup>18</sup> On the basis of PM-IRAS data, the authors propose that a  $(3 \times 3)$ -7NO structure with an NO coverage of 7/9 monolayer (ML) is also formed at elevated NO pressures on the Pd(111) surface. As for Rh(111), this structure has never been observed at lower pressures and temperatures for which the highest-coverage NO structure is the  $(2 \times 2)$ -3NO structure with a coverage of 3/4 ML.<sup>19–23</sup> However, the evidence for the  $(3 \times 3)$  structure from vibrational spectroscopy is indirect with respect to a genuine structural determination. We therefore decided to complement these PM-IRAS data with HP-STM data to explore the existence of a  $(3 \times 3)$ -7NO adsorption structure.

In the present letter, we find from atomically resolved STM experiments that at room temperature and high NO pressures of up to 720 Torr only the  $(2 \times 2)$ -3NO structure is formed. The STM results are supported by state-of-the-art ab initio DFT calculations. We therefore conclude that the NO/Pd(111) system does not provide a pressure gap between standard low-pressure conditions and high-pressure conditions. The origin of the apparent discrepancy of the present STM and DFT results with the recent PM-IRAS data will be briefly discussed.

The experiments were performed in a combined UHV and high-pressure (HP) system comprising a UHV chamber (base pressure  $\approx 1 \times 10^{-10}$  Torr) equipped with the home-built

\* To whom correspondence should be addressed. E-mail: fbe@inano.dk.

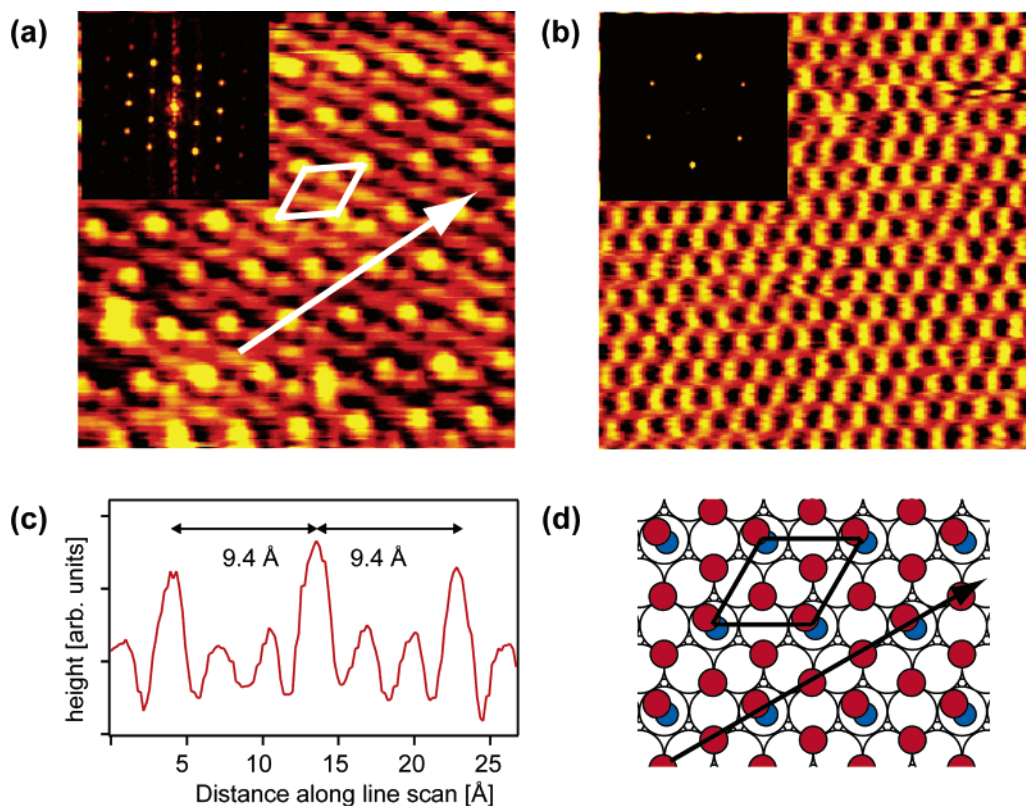


**Figure 1.** (a) STM image ( $41 \times 41 \text{ Å}^2$ ) of NO on Pd(111) obtained at room temperature in a background of 720 Torr of NO; the  $(2 \times 2)$  unit cell and a line scan direction are indicated (small insert: 2D Fourier transform). (b) STM image ( $41 \times 41 \text{ Å}^2$ ) of a clean Pd(111) surface (small insert: 2D Fourier transform). (c) Line scan showing the three NO molecules in the unit cell; atop adsorbed NO is clearly distinguished from threefold hollow site adsorbed NO by their different apparent heights. (d) Ball model of the  $p(2 \times 2)$ -3NO structure on Pd(111) (oxygen atoms are red, and nitrogen atoms are blue). The  $(2 \times 2)$  unit cell and line scan direction corresponding to those in the STM image are indicated.

Aarhus STM<sup>24</sup> and standard surface analysis tools. The sample can be transferred under UHV conditions from the main chamber to a separate HP cell equipped with a home-built in situ HP-STM with a design similar to the Aarhus STM.<sup>25</sup> Through a gas-handling system, the HP cell can be filled with up to 1 atm of a mixture of ultra-clean gases, and STM images can be obtained in situ. The inner parts of the HP cell as well as the metal parts of the STM are gold-coated in order to avoid any reactions occurring on the chamber walls at the high-pressure conditions. High-purity NO (Messer 99.5%) was used for the NO exposure experiments; further purification, which is important for HP studies, was performed by leading the gas through a copper coil submerged in an ethanol slush kept at approximately  $-100^\circ\text{C}$  during the gas inlet.

The Pd(111) single crystal was cleaned by sputtering (1 keV) and annealing (900 K) cycles, and the cleanliness was confirmed by STM images showing a  $(1 \times 1)$  Pd(111) structure with no impurities. Although the STM has no chemical specificity, it offers a higher sensitivity than almost all other techniques, and even individual impurities (e.g., at the step edges) can easily be detected from high-resolution STM images.

The DFT calculations were performed using the DACAPO code with ultrasoft pseudopotential and a plane-wave basis set (cutoff energy 25 Rydbergs).<sup>26</sup> Exchange-correlation (XC) effects were described with the GGA-RPBE functional.<sup>26</sup> The Pd(111) surface was modeled by a four-layer slab. The two lower Pd layers were kept fixed, whereas the upper two layers and the NO molecules were relaxed until the total sum of residual forces was below  $0.05 \text{ eV/Å}$ . In this study, we investigated two structures,  $(2 \times 2)$ -3NO and  $(3 \times 3)$ -7NO, corresponding to  $3/4$  ML and  $7/9$  ML NO coverages, respectively. The  $k$ -points meshes of the surface Brillouin-zone

integration were  $6 \times 6$  and  $4 \times 4$ , respectively. In addition to the DFT results, which can be regarded as zero-temperature, zero-pressure findings, we used statistical mechanics to calculate the  $(T, p)$  phase diagram.<sup>27,28</sup> The chemical potential of all of the related surface species are functionals of the temperature  $T$  and pressure  $p$ , and by determining the  $(T, p)$  phase diagram, information on the adsorption phases from UHV to high-pressure conditions was obtained, whereby we are able to bridge the pressure gap. The surface free energy of a certain surface species can be defined as

$$\gamma(T, p) = (G_{\text{NO/Pd(111)}} - G_{\text{Pd(111)}} - N\mu_{\text{NO}})/A \quad (1)$$

The  $G_{\text{NO/Pd(111)}}$  and  $G_{\text{Pd(111)}}$  are the free energies of the investigated NO/Pd surface species and the clean Pd(111) reference system. They can be replaced by the DFT calculated total energies  $E_{\text{NO/Pd(111)}}$  and  $E_{\text{Pd(111)}}$ , since the vibrational and entropic contributions of  $G_{\text{NO/Pd(111)}}$  and  $G_{\text{Pd(111)}}$  are very small. The chemical potential of NO is dependent on the temperature and pressure and is given by

$$\mu_{\text{NO}} = E_{\text{NO}}^{\text{total}} + \tilde{\mu}_{\text{NO}}(T, P^0) + k_{\text{B}}T \ln\left(\frac{P_{\text{NO}}}{P^0}\right) \quad (2)$$

$P^0$  is the atmospheric pressure, and  $\tilde{\mu}_{\text{NO}}(T, P^0)$  includes the contribution from rotation and vibration of the molecule, as well as the ideal-gas entropy at 1 atm. Finally, we define  $\Delta\mu_{\text{NO}}$  as  $\mu_{\text{NO}} - E_{\text{NO}}^{\text{total}}$ . All of the experimental values were taken from the JANAF thermochemical tables.<sup>29</sup>

The NO adsorption structure was explored by in situ scanning at room temperature in a background pressure of NO. Figure 1a shows an STM image obtained at an NO pressure of 720

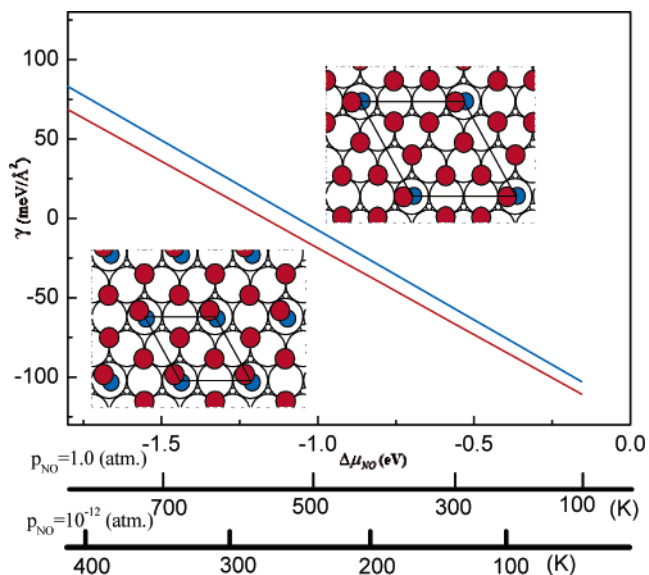
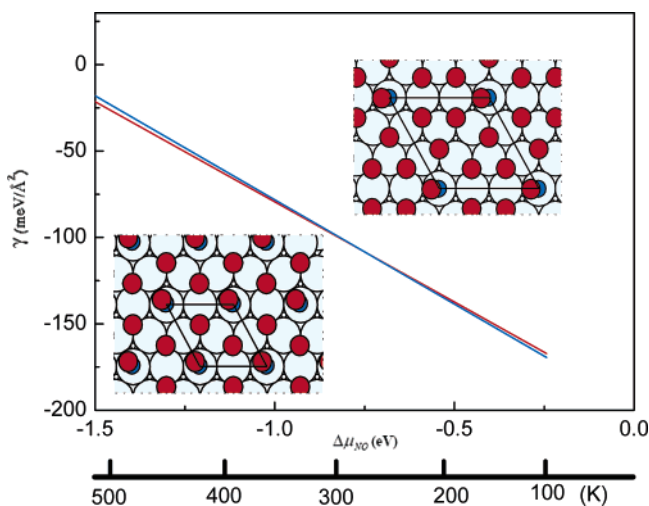
**TABLE 1: Chemisorption Energies and Structural Parameters for the  $(2 \times 2)$ -3NO and  $(3 \times 3)$ -7NO Adsorption Structures on Rh(111) and Pd(111)**

	Rh(111)		Pd(111)	
	$(2 \times 2)$ -3NO	$(3 \times 3)$ -7NO	$(2 \times 2)$ -3NO	$(3 \times 3)$ -7NO
$E_{\text{ads}}$ (eV/per NO)	1.68	1.65	1.17	1.07
$d_{(\text{metal}-\text{N})}$ ( $\text{\AA}$ )-atop	1.78	1.80	1.98	1.98
$d_{(\text{metal}-\text{N})}$ ( $\text{\AA}$ )-fcc	2.07–2.08	2.04–2.12	2.12–2.14	2.10–2.17
$d_{(\text{metal}-\text{N})}$ ( $\text{\AA}$ )-hcp	2.05–2.08	2.04–2.14	2.10–2.12	2.15–2.20
$\alpha_{\text{Pd}-\text{N}-\text{O-atop}}$	163°	153°	129°	130°

Torr. A hexagonal pattern of bright protrusions is observed in this STM image (the unit cell is indicated with white lines). The STM was calibrated from high-resolution images of the clean Pd(111) surface (see Figure 1b), and from a detailed comparison of the close-packed directions and nearest-neighbor distances on the clean Pd(111) surface, we conclude that the hexagonal structure formed upon HP NO exposure fits nicely with a  $(2 \times 2)$  structure. The  $(2 \times 2)$  structure is also very distinct in the comparison of the 2D Fourier transform of the NO adsorption structure and of the clean Pd(111) surface (see the small inserts in Figure 1a,b). In the line scan in Figure 1c, the distance between two adjacent bright protrusions is measured to be 9.4  $\text{\AA}$ , which is very close to the ideal distance of  $\sqrt{12} \times 2.76 \text{ \AA} = 9.56 \text{ \AA}$  for a  $(2 \times 2)$  structure on Pd(111) (Pd–Pd nearest neighbor distance = 2.76  $\text{\AA}$ ). We then conclude that the observed NO adsorption structure fits with a  $(2 \times 2)$  structure within the uncertainty of the calibration of the STM (a few percent).

A similar  $(2 \times 2)$ -3NO structure is observed at low pressure and low temperature. This structure has been studied by STM, HREELS, IR vibrational spectroscopy, LEED, UPS, TDS, work function measurements, and DFT calculations and is characterized as a  $(2 \times 2)$ -3NO structure with a 1:2 mixture of tilted atop and threefold hollow-site adsorbed NO with an NO coverage of 3/4 ML.<sup>19–23</sup> A ball model of this  $(2 \times 2)$ -3NO structure is shown in Figure 1d with a  $(2 \times 2)$  unit cell superimposed. By comparing this to the structure observed by STM in Figure 1a, it is evident that the bright protrusions in the STM image can be associated with the tilted atop adsorbed NO molecules. Furthermore, it is evident from the line scan in Figure 1c that we can distinguish two types of protrusions in the STM image by their different apparent heights. A line scan along the same direction is also indicated in the ball model, and this shows that the less bright protrusions coincide with the threefold hollow-site adsorbed NO molecules. We performed experiments at several NO pressures ranging from 200 Torr to 720 Torr, and we never observed any other structures than the  $p(2 \times 2)$ -3NO. On the basis of our STM measurements, we thus conclude that the  $(2 \times 2)$ -3NO adsorption structure is the only one formed at room temperature and up to 720 Torr NO pressure.

To confirm that the  $(2 \times 2)$ -3NO structure indeed is more stable than the  $(3 \times 3)$ -7NO structure proposed by Ozensoy et al. at the pressure and temperature conditions of our experiments, we performed DFT calculations for these two adsorption structures. From the calculations, we found the adsorption energies per NO molecule to be  $-1.17 \text{ eV}$  and  $-1.07 \text{ eV}$  for the  $(2 \times 2)$ -3NO and  $(3 \times 3)$ -7NO structures, respectively (the results of the DFT calculations are summarized in Table 1). The adsorption energy for the  $(2 \times 2)$ -3NO structure is consistent with results reported from our group in a previous study, in which several ordered structures formed under UHV conditions were characterized by STM and DFT.<sup>23</sup> The lower adsorption energy per NO molecule indicates that theory also finds the  $(2 \times 2)$ -3NO structure to be the most stable one. A

**Figure 2.** Surface free energies for the  $(2 \times 2)$ -3NO (red line) and  $(3 \times 3)$ -7NO (blue line) adsorption structures on Pd(111). Temperature axes are shown for NO pressures of 1 atm and  $1 \times 10^{-12}$  atmosphere.**Figure 3.** Surface free energies for the  $(2 \times 2)$ -3NO (red line) and  $(3 \times 3)$ -7NO (blue line) adsorption structures on Rh(111). Temperature axis is shown for an NO pressure of 0.03 Torr.

similar conclusion is in fact also reached in the theoretical part of the paper of Ozensoy et al.<sup>18</sup> As mentioned earlier, the DFT calculations assume zero temperature and pressure and are, thus, not directly compatible with our experimental results. To extend the theoretical results to the experimental conditions, we calculated the surface free energies for the two NO adsorption structures. The results of these calculations are shown in Figure 2, from which we conclude that the  $(3 \times 3)$ -7NO is unstable for all practical temperature and pressure conditions. In particular, we find that the free surface energy of the  $(2 \times 2)$ -3NO structure is 9.46  $\text{meV}/\text{\AA}^2$  lower than that of the  $(3 \times 3)$ -7NO structure at the conditions of our STM measurements (300 K and 720 torr NO pressure).

The validity of the DFT calculations was judged by performing similar calculations for the  $(2 \times 2)$ -3NO and  $(3 \times 3)$ -7NO adsorption structures on Rh(111) to investigate whether these calculations are in agreement with the experimental findings of Rider et al.<sup>7</sup> The free energy diagram (Figure 3) indeed shows that for Rh(111) the  $(3 \times 3)$ -7NO adsorption structure becomes thermodynamically favored at high NO chemical potential. At



an NO pressure of 0.03 Torr, we find that the transition temperature between the two structures is very close to room temperature. This is in excellent agreement with the results of Rider et al.<sup>7</sup> and provides strong support to the validity of the DFT calculational scheme. The results of the DFT calculations also suggest an explanation for the different behavior of NO adsorption on Pd(111) vs Rh(111). The absolute binding energies per NO molecule are significantly higher on Rh(111) than on Pd(111) for both the (2 × 2) structure (1.68 eV vs 1.17 eV) and the (3 × 3) structure (1.65 eV vs 1.07 eV). This implies that NO is more likely to form higher-coverage structures on Rh(111) than on Pd(111), thus rationalizing the experimental findings in the present work and the work of Rider et al.

From our results, we find no direct explanation as to why the PM-IRAS spectrum changes at high NO pressure, as observed by Ozensoy et al.<sup>18</sup> On the basis of the present STM and DFT results, we discard the proposed (3 × 3)-7NO adsorption structure, and it therefore still remains to be settled how to interpret these PM-IRAS data. In conclusion, we find strong evidence from both STM and DFT that the most stable adsorption structure of NO on Pd(111) at room temperature and 720 Torr is the (2 × 2)-3NO structure, and thus, no pressure gap exists between high-pressure and standard low-pressure conditions.

**Acknowledgment.** Prof. D. Wayne Goodman is acknowledged for stimulating discussions. The Danish Research Councils and Dansk Center for Scientific Computing are acknowledged for financial and computational support.

## References and Notes

- (1) Somorjai, G. A. *Introduction to Surface Chemistry and Catalysis*; John Wiley & Sons: New York, 1994.
- (2) Ertl, G. *Angew. Chem., Int. Ed. Engl.* **1990**, 29, 1219.
- (3) Thostrup, P.; Vestergaard, E. K.; An, T.; Lægsgaard, E.; Besenbacher, F. *J. Chem. Phys.* **2003**, 118, 3724.
- (4) Longwitz, S. R.; Schnadt, J.; Vestergaard, E. K.; Vang, R. T.; Lægsgaard, E.; Stensgaard, I.; Brune, H.; Besenbacher, F. *J. Phys. Chem. B* **2004**, 108, 14497.
- (5) Vestergaard, E. K.; Thostrup, P.; An, T.; Lægsgaard, E.; Stensgaard, I.; Hammer, B.; Besenbacher, F. *Phys. Rev. Lett.* **2002**, 88, 259601.
- (6) Hendriksen, B. L. M.; Frenken, J. W. M. *Phys. Rev. Lett.* **2002**, 89.
- (7) Rider, K. B.; Hwang, K. S.; Salmeron, M.; Somorjai, G. A. *Phys. Rev. Lett.* **2001**, 86, 4330.
- (8) Osterlund, L.; Rasmussen, P. B.; Thostrup, P.; Lægsgaard, E.; Stensgaard, I.; Besenbacher, F. *Phys. Rev. Lett.* **2001**, 86, 460.
- (9) Hansen, P. L.; Wagner, J. B.; Helveg, S.; Rostrup-Nielsen, J. R.; Clausen, B. S.; Topsøe, H. *Science* **2002**, 295, 2053.
- (10) Peters, K. F.; Walker, C. J.; Steadman, P.; Robach, O.; Isern, H.; Ferrer, S. *Phys. Rev. Lett.* **2001**, 86, 5325.
- (11) Rupprechter, G.; Dellwig, T.; Unterhalt, H.; Freund, H. J. *J. Phys. Chem. B* **2001**, 105, 3797.
- (12) Ozensoy, E.; Hess, C.; Goodman, D. W. *Top. Catal.* **2004**, 28, 13.
- (13) Villegas, I.; Weaver, M. J. *J. Chem. Phys.* **1994**, 101, 1648.
- (14) Li, W. X.; Österlund, L.; Vestergaard, E. K.; Vang, R. T.; Matthiesen, J.; Pedersen, T. M.; Lægsgaard, E.; Hammer, B.; Besenbacher, F. *Phys. Rev. Lett.* **2004**, 93, 146104.
- (15) Over, H.; Muhler, M. *Prog. Surf. Sci.* **2003**, 72, 3.
- (16) Nerlov, J.; Sckerl, S.; Wambach, J.; Chorkendorff, I. *Appl. Catal., A* **2000**, 191, 97.
- (17) Christoffersen, E.; Liu, P.; Ruban, A.; Skriver, H. L.; Nørskov, J. K. *J. Catal.* **2001**, 199, 123.
- (18) Ozensoy, E.; Hess, C.; Loffreda, D.; Sautet, P.; Goodman, D. W. *J. Phys. Chem. B* **2005**, 109, 5414.
- (19) Loffreda, D.; Simon, D.; Sautet, P. *Chem. Phys. Lett.* **1998**, 291, 15.
- (20) Conrad, H.; Ertl, G.; Kuppers, J.; Latta, E. E. *Surf. Sci.* **1977**, 65, 235.
- (21) Chen, P. J.; Goodman, D. W. *Surf. Sci.* **1993**, 297, L93.
- (22) Bertolo, M.; Jacobi, K. *Surf. Sci.* **1990**, 226, 207.
- (23) Hansen, K. H.; Slijivancanin, Z.; Hammer, B.; Lægsgaard, E.; Besenbacher, F.; Stensgaard, I. *Surf. Sci.* **2002**, 496, 1.
- (24) Lægsgaard, E.; Besenbacher, F.; Mortensen, K.; Stensgaard, I. *J. Microsc. (Oxford, UK)* **1988**, 152, 663.
- (25) Lægsgaard, E.; Österlund, L.; Thostrup, P.; Rasmussen, P. B.; Stensgaard, I.; Besenbacher, F. *Rev. Sci. Instrum.* **2001**, 72, 3537.
- (26) Hammer, B.; Hansen, L. B.; Nørskov, J. K. *Phys. Rev. B* **1999**, 59, 7413.
- (27) Reuter, K.; Scheffler, M. *Phys. Rev. B* **2003**, 68, 045407.
- (28) Reuter, K.; Scheffler, M. *Phys. Rev. Lett.* **2003**, 90, 046103.
- (29) Chase, M. W. *NIST-JANAF Thermochemical Tables*, 4th ed.; American Chemical Society: Washington, DC, 1998.